



# Substituent dependent topologies in cobalt isophthalate coordination polymers with bis(pyridylmethyl)piperazine coligands

Amy M. Pochodylo, Robert L. LaDuca\*

Lyman Briggs College and Department of Chemistry, Michigan State University, East Lansing, MI 48825, USA

## ARTICLE INFO

### Article history:

Received 5 October 2010  
Received in revised form 21 February 2011  
Accepted 3 March 2011  
Available online 16 March 2011

### Keywords:

Cobalt  
Dicarboxylate  
Coordination polymer  
Hydrogen bonding  
Ferromagnetism

## ABSTRACT

Divalent cobalt coordination polymers containing bis(4-pyridylmethyl)piperazine (4-bpmp) or bis(3-pyridylmethyl)piperazine (3-bpmp) ligands and 5-substituted isophthalate ligands have been hydrothermally prepared and structurally characterized by single-crystal X-ray diffraction.  $[\text{Co}(\text{OHip})(4\text{-bpmp})]_n$  (**1**, OHip = 5-hydroxyisophthalate) manifests a (4,4) grid 2D coordination polymer structure, with *anti-syn* bridged  $\{\text{Co}_2(\text{OCO})_2\}$  dimers serving as connecting nodes. Similar dinuclear  $\{\text{Co}_2(\text{OCO})_2\}$  clusters are evident in  $[\text{Co}(\text{OMeip})(4\text{-bpmp})]_n$  (**2**, OMeip = 5-methoxyisophthalate). However, the lack of hydrogen-bonding capability of the methoxy substituent promotes formation of a rarer 6-connected (3,6) triangular net.  $\{[\text{Co}(\text{H}_2\text{O})_4(\text{H}_2\text{3-bpmp})](\text{NO}_2\text{ip})_2 \cdot 6\text{H}_2\text{O}\}_n$  (**3**, NO<sub>2</sub>ip = 5-nitroisophthalate) possesses cationic  $[\text{Co}(\text{H}_2\text{O})_4(\text{H}_2\text{3-bpmp})]_n^{4n+}$  chains connected into a supramolecular lattice by unligated NO<sub>2</sub>ip dianions and water molecules of crystallization. The variable temperature magnetic susceptibility behavior of **1** and **2** is ascribed to cooperation between single-ion effects and weak ferromagnetic superexchange.

© 2011 Elsevier B.V. All rights reserved.

## 1. Introduction

Crystalline coordination polymer solids possess important industrially focused applications [1,2] such as gas storage [3], selective absorption and separation [4], ion exchange [5], heterogeneous catalysis [6], luminescence [7], and non-linear optical behavior [8]. Aromatic dicarboxylates such as terephthalate [9] or isophthalate (ip) [10] are commonly employed ligands in the molecular design of divalent metal coordination polymers, because they can impart a rigid crystalline framework and necessary charge balance. Interplay between metal ion coordination preference, geometric disposition of the carboxylate groups on the aromatic ring, carboxylate binding mode and the inclusion of any dipodal nitrogen-base tethering ligands [11] induces diverse structural topologies in these systems, although *a priori* prediction of coordination polymer structure remains elusive in most cases. In coordination polymer solids containing divalent cobalt ions, the presence of multinuclear clusters or cobalt carboxylate chains can result in intriguing magnetic behavior including spin-canting and single-chain magnetism [12].

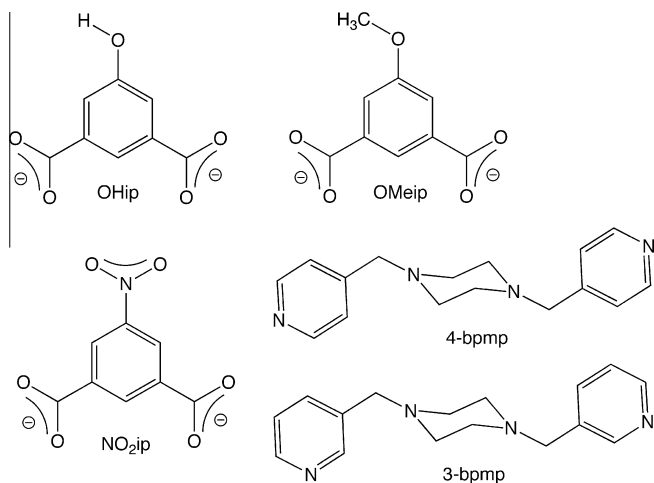
Isophthalate ligand derivatives with substituents at their mutually *meta*-disposed 5-positions, such as 5-hydroxyisophthalate (OHip) [13–16], 5-methoxyisophthalate (OMeip) [17,18], and 5-nitroisophthalate (NO<sub>2</sub>ip) [19–23] (Scheme 1), have been used

in tandem with dipyriddy nitrogen-base co-ligands in order to augment in these materials topological diversity. For instance,  $\{[\text{Co}(\text{OHip})(\text{dpp})] \cdot \text{H}_2\text{O}\}_n$  (dpp = 1,3-di(4-pyridyl)propane) shows a fourfold interpenetrated diamondoid topology, while its nickel derivative  $[\text{Ni}(\text{OHip})(\text{dpp})_{1.5}(\text{H}_2\text{O})]_n$  displays interdigitated sets of 1D ribbon motifs [13].  $\{[\text{Co}(\text{3-bpt})(\text{NO}_2\text{ip})(\text{H}_2\text{O})_2] \cdot (\text{H}_2\text{O})\}_n$  (3-bpt = 4-amino-3,5-bis(3-pyridyl)-1,2,4-triazole) has a simple (4,4) grid topology [19] but  $\{[\text{Co}(\text{NO}_2\text{ip})(\text{dpee})] \cdot 0.5\text{dpee} \cdot \text{H}_2\text{O}\}_n$  (dpee = 1,2-di(4-pyridyl)ethylene) exhibits a 2D bilayer structure with nanoscale rectangular channels that encapsulate organic species [20]. Despite some exploratory synthesis of individual coordination polymer phases, studies that systematically investigate size-dependent steric effects imparted by substituted isophthalate ligands on coordination polymer topology have been less common, especially in divalent cobalt systems. Yang and co-workers performed one such study in a divalent zinc system [24], preparing the coordination polymers  $[\text{Zn}_4(\text{H}_2\text{O})(\text{isophthalate})_4(\text{py})_6]_n$  (py = pyridine),  $\{[\text{Zn}_2(\text{OHip})_2(\text{py})_4]_2 \cdot (\text{py})\}_n$ , and  $[\text{Zn}(\text{tBuip})(\text{py})_2]_n$  (tBuip = 5-*tert*-butylisophthalate). In this series increasing the steric hindrance imparted by the 5-position substituent caused a decrease in coordination polymer dimensionality, from a 2D grid-like layer to 1D single- and double-stranded chains.

In this study we have investigated the preparation of divalent cobalt coordination polymers containing a 5-position substituted isophthalate ligand and bis(pyridylmethyl)piperazine (bpmp) isomers 3-bpmp or 4-bpmp (Scheme 1). The 4-bpmp ligand has afforded topologically interesting nets such as the 8-connected  $4^4 5^1 7^6$  self-penetrated net in  $[\text{Co}_3(\text{oba})_3(4\text{-bpmp})_2]_n$  (oba = oxybisbenzoate)

\* Corresponding author. Address: Lyman Briggs College, E-30 Holmes Hall, Michigan State University, East Lansing, MI 48825, USA. Tel.: +1 517 432 2268.

E-mail addresses: laduca@msu.edu, laduca@chemistry.msu.edu (R.L. LaDuca).



Scheme 1. Ligands used in this study.

[25] and the rare threaded-loop self-penetrated layer seen in  $\{[\text{Zn}_3(\text{tca})_2(4\text{-bpmp})(\text{H-}4\text{-bpmp})_2](\text{ClO}_4)_2 \cdot 5\text{H}_2\text{O}\}_n$  ( $\text{tca}$  = tricarbalate) [26]. Although the 3-bpmp ligand has tended to promote lower dimensionalities [27], it has allowed generation of some rare 3D networks [28]. We report here the synthesis and structural characterization of the coordination polymer solids  $[\text{Co}(\text{OHip})(4\text{-bpmp})]_n$  (**1**) and  $[\text{Co}(\text{OMeip})(4\text{-bpmp})]_n$  (**2**), whose topologies depend critically on the steric bulk and hydrogen bonding capability of the isophthalate 5-position substituent. A series of attempts were undertaken to prepare divalent cobalt substituted isophthalate coordination polymers containing the isomeric 3-bpmp ligand, in order to explore the effect of nitrogen donor geometric disposition. Unfortunately only  $\text{H}_2\text{NO}_2\text{ip}$  afforded any crystalline product, resulting in the isolation of the 1D chain complex  $\{[\text{Co}(\text{H}_2\text{O})_4(\text{H}_2\text{3-bpmp})](\text{NO}_2\text{ip})_2 \cdot 6\text{H}_2\text{O}\}_n$  (**3**). Magnetic superexchange and single-ion effects within the dinuclear units formed in compounds **1** and **2** were also investigated.

## 2. Experimental

### 2.1. General considerations

Cobalt salts and substituted isophthalic acids were obtained commercially from Aldrich. Bis(4-pyridylmethyl)piperazine (4-bpmp) and bis(3-pyridylmethyl)piperazine (3-bpmp) were prepared via modification of a published procedure [29]. Water was deionized above 3 MΩ cm in-house. Elemental analysis was performed by Micro-Analysis, Inc., Wilmington, Delaware, USA. IR spectra Infrared spectra were recorded on powdered samples on a Perkin Elmer Spectrum One instrument. Variable temperature magnetic susceptibility data (2 K to 300 K) for **1** and **2** were collected on a Quantum Design MPMS SQUID magnetometer at an applied field of 0.1 T. After each temperature change the sample was kept at the new temperature for 5 min before magnetization measurement to ensure thermal equilibrium. The susceptibility data was corrected for diamagnetism using Pascal's constants and for the diamagnetism of the sample holder [30].

### 2.2. Preparation of $[\text{Co}(\text{OHip})(4\text{-bpmp})]_n$ (**1**)

$\text{Co}(\text{NO}_3)_2 \cdot 6\text{H}_2\text{O}$  (108 mg, 0.369 mmol), 4-bpmp (99 mg, 0.37 mmol), 5-hydroxyisophthalic acid (67 mg, 0.37 mmol) and 10 mL deionized water were placed into a 23 mL Teflon-lined acid digestion bomb, along with 1.0 mL of a 1.0 M NaOH solution. The bomb was sealed and heated in an oven at 120 °C for 72 h, and then

cooled slowly to 25 °C. Magenta blocks of **1** (48 mg, 26% yield based on Co) were isolated after washing with distilled water, ethanol, and acetone and drying in air. *Anal. Calc.* for  $\text{C}_{48}\text{H}_{48}\text{Co}_2\text{N}_8\text{O}_{10}$  **1**: C, 56.81; H, 4.77; N, 11.04. Found: C, 56.55; H, 4.29; N, 10.85%. IR ( $\text{cm}^{-1}$ ): 3300 (w, br), 3079 (w), 2940 (w), 2818 (w), 1616 (w), 1582 (s), 1532 (m), 1456 (m), 1422 (m), 1380 (s), 1347 (w), 1319 (w), 1296 (w), 1272 (w), 1231 (w), 1158 (m), 1133 (m), 1066 (w), 1010 (s), 975 (m), 931 (w), 888 (w), 838 (m), 817 (w), 799 (w), 784 (s), 722 (s), 670 (w).

### 2.3. Preparation of $[\text{Co}(\text{OMeip})(4\text{-bpmp})]_n$ (**2**)

$\text{Co}(\text{NO}_3)_2 \cdot 6\text{H}_2\text{O}$  (108 mg, 0.369 mmol), 4-bpmp (99 mg, 0.37 mmol), 5-methoxyisophthalic acid (73 mg, 0.37 mmol) and 10 mL deionized water were placed into a 23 mL Teflon-lined acid digestion bomb. The bomb was sealed and heated in an oven at 120 °C for 48 h, and then cooled slowly to 25 °C. Magenta blocks of **2** (18 mg, 9% yield based on Co) were isolated after washing with distilled water, ethanol, and acetone and drying in air. *Anal. Calc.* for  $\text{C}_{25}\text{H}_{23}\text{CoN}_4\text{O}_5$  **2**: C, 57.59; H, 5.03; N, 10.74. Found: C, 57.78; H, 4.94; N, 10.43%. IR ( $\text{cm}^{-1}$ ): 3047 (w), 2941 (w), 2816 (w), 1620 (w), 1579 (s), 1540 (w), 1456 (s), 1412 (m), 1385 (s), 1344 (w), 1322 (w), 1293 (m), 1267 (m), 1231 (w), 1151 (w), 1130 (s), 1060 (s), 1008 (s), 942 (w), 924 (s), 889 (w), 858 (w), 840 (m), 816 (w), 787 (s), 721 (s), 669 (w).

### 2.4. Preparation of $\{[\text{Co}(\text{H}_2\text{O})_4(\text{H}_2\text{3-bpmp})](\text{NO}_2\text{ip})_2 \cdot 6\text{H}_2\text{O}\}_n$

$\text{Co}(\text{NO}_3)_2 \cdot 6\text{H}_2\text{O}$  (108 mg, 0.369 mmol), 3-bpmp (99 mg, 0.37 mmol), 5-nitroisophthalic acid (78 mg, 0.37 mmol) and 10 mL deionized water were placed into a 23 mL Teflon-lined acid digestion bomb. The bomb was sealed and heated in an oven at 120 °C for 48 h, and then cooled slowly to 25 °C. Pink blocks of **3** (101 mg, 30% yield based on the acid) were isolated after washing with distilled water, ethanol, and acetone and drying in air. *Anal. Calc.* for  $\text{C}_{32}\text{H}_{48}\text{CoN}_6\text{O}_{22}$  **3**: C, 41.43; H, 5.22; N, 10.74. Found: C, 41.98; H, 4.78; N, 11.10%. IR ( $\text{cm}^{-1}$ ): 3300 (w, br), 2994 (w, br), 2357 (w), 1598 (s), 1530 (s), 1452 (m), 1437 (w), 1418 (w), 1361 (w), 1344 (s), 1277 (w), 1197 (w), 1092 (w), 1071 (m), 1043 (w), 989 (w), 958 (w), 931 (m), 916 (w), 846 (w), 789 (s), 756 (w), 732 (m), 698 (s).

## 3. X-ray crystallography

Single-crystal reflection data for **1–3** were collected using a Bruker-AXS Apex2 CCD instrument. Reflection data was acquired using graphite-monochromated Mo  $K\alpha$  radiation ( $\lambda = 0.71073 \text{ \AA}$ ). The reflection data were integrated with SAINT [31]. Lorentz and polarization effect and empirical absorption corrections were applied with SADABS [32]. The structures were solved using direct methods and refined on  $F^2$  using SHELXL [33]. All non-hydrogen atoms were refined with anisotropic thermal parameters. Hydrogen atoms bound to carbon atoms were placed in calculated positions and refined with isotropic thermal parameters using a riding model. Hydrogen atoms bound to water molecules were located by Fourier difference map and restrained at fixed positions. Relevant crystallographic data for **1–3** are listed in Table 1.

## 4. Results and discussion

### 4.1. Synthesis and spectral characterization

Hydrothermal reaction of cobalt nitrate, the requisite dicarboxylic acid, and the appropriate bis(pyridylmethyl)piperazine isomer generated crystalline samples of **1–3**. The infrared spectra of **1–3**

**Table 1**  
Crystal and structure refinement data for **1–3**.

Compound	<b>1</b>	<b>2</b>	<b>3</b>
Empirical formula	C <sub>48</sub> H <sub>48</sub> Co <sub>2</sub> N <sub>8</sub> O <sub>10</sub>	C <sub>25</sub> H <sub>26</sub> CoN <sub>4</sub> O <sub>5</sub>	C <sub>32</sub> H <sub>48</sub> CoN <sub>6</sub> O <sub>22</sub>
Formula weight	1014.80	521.43	927.69
Crystal system	triclinic	monoclinic	triclinic
Space group	<i>P</i> $\bar{1}$	<i>P</i> 2 <sub>1</sub> / <i>c</i>	<i>P</i> $\bar{1}$
<i>a</i> (Å)	11.6902(9)	12.670(3)	8.6581(7)
<i>b</i> (Å)	13.6397(10)	10.095(3)	10.5948(9)
<i>c</i> (Å)	14.0927(10)	18.237(5)	11.1721(9)
$\alpha$ (°)	87.051(1)	90	75.964(1)
$\beta$ (°)	89.268(1)	91.786(4)	83.826(1)
$\gamma$ (°)	80.615(1)	90	89.243(1)
<i>V</i> (Å <sup>3</sup> )	2214.1(3)	2331.5(10)	988.37(14)
<i>Z</i>	2	4	1
<i>D</i> <sub>calc</sub> (g cm <sup>-3</sup> )	1.522	1.485	1.559
$\mu$ (mm <sup>-1</sup> )	0.821	0.781	0.530
Minimum/maximum transmission	0.8889/0.9524	0.8179/0.9052	0.9101/0.9679
<i>hkl</i> ranges	-14 ≤ <i>h</i> ≤ 14, -16 ≤ <i>k</i> ≤ 16, -16 ≤ <i>l</i> ≤ 16	-15 ≤ <i>h</i> ≤ 15, -11 ≤ <i>k</i> ≤ 11, -21 ≤ <i>l</i> ≤ 21	-10 ≤ <i>h</i> ≤ 10, -12 ≤ <i>k</i> ≤ 12, -13 ≤ <i>l</i> ≤ 13
Total reflections	32 441	13 778	14 345
Unique reflections	8056	4153	3590
<i>R</i> <sub>int</sub>	0.0714	0.0458	0.0613
Parameters/restraints	619/0	317/0	298/16
<i>R</i> <sub>1</sub> (all data) <sup>a</sup>	0.0694	0.0542	0.0901
<i>R</i> <sub>1</sub> ( <i>I</i> > 2σ( <i>I</i> )) <sup>a</sup>	0.0447	0.0434	0.0708
<i>wR</i> <sub>2</sub> (all data) <sup>b</sup>	0.1237	0.1205	0.2002
<i>wR</i> <sub>2</sub> ( <i>I</i> > 2σ( <i>I</i> )) <sup>b</sup>	0.1092	0.1124	0.1825
Maximum/minimum residual (e <sup>-</sup> /Å <sup>3</sup> )	0.303/-0.603	0.500/-0.684	1.331/-1.453
Goodness-of-fit (GOF)	1.040	1.063	1.078

<sup>a</sup>  $R_1 = \sum ||F_o| - |F_c|| / \sum |F_o|$ .<sup>b</sup>  $wR_2 = \{ \sum [w(F_o^2 - F_c^2)^2] / \sum [wF_o^2] \}^{1/2}$ .

were consistent with their single crystal structures. Medium intensity bands in the range of ~1600–~1200 cm<sup>-1</sup> are attributed to stretching modes of the pyridyl rings of the bpmp ligands and the aromatic rings of the substituted isophthalate ligands. Features corresponding to pyridyl ring puckering modes are evident in the region between ~930 and ~600 cm<sup>-1</sup>. Asymmetric and symmetric C–O stretching modes of the fully deprotonated dicarboxylate ligands are present as strong bands at 1531 and 1380 cm<sup>-1</sup> (**1**), 1579 and 1385 cm<sup>-1</sup> (**2**), and 1530 and 1360 cm<sup>-1</sup> (**3**). Broad, weak spectral features at ~3400 cm<sup>-1</sup> for **1** and **3** denote the presence of O–H stretching modes in the bound or unbound water molecules, or the hydroxy group in **1**. The nitro substituent in **3** is evidenced by a strong N–O stretching band at 1343 cm<sup>-1</sup>.

#### 4.2. Structural description of [Co(OHip)(4-bpmp)]<sub>n</sub> (**1**)

The asymmetric unit of compound **1** contains two crystallographically distinct divalent cobalt atoms, two doubly deprotonated OHip ligands, and two 4-bpmp ligands. About each cobalt atom, the coordination environment is a distorted {CoN<sub>2</sub>O<sub>3</sub>} square pyramid with pyridyl nitrogen donor atoms from two 4-bpmp ligands occupying *trans* positions within the basal plane. Oxygen donor atoms from three different OHip ligands fill the remaining three coordination sites. Different deviations from idealized square pyramidal geometry ( $\tau = 0.445$  and 0.347 for Co1 and Co2, respectively [34]) enforce the crystallographic distinction between the cobalt atoms. Weaker semi-ligating interactions [35] between OHip carboxylate oxygen atoms and cobalt (Co1...O1, 2.578 Å; Co2...O8, 2.431 Å) give rise to “5+1” expanded secondary coordination environments. Relevant bond information for **1** is listed in Table 2.

Each OHip moiety bridges three cobalt atoms in a  $\kappa^3$ O:O':O'' ligating mode, with one of its carboxylate arms linking a Co1 and a Co2 atom in an *anti-syn* arrangement. Pairs of Co1 and Co2 atoms are linked by two *anti-syn* carboxylate bridges to construct {Co<sub>2</sub>

**Table 2**  
Bond length (Å) and angle (°) data for **1**.

Co1–O2 <sup>#1</sup>	2.013(2)	O3–Co1–N1	88.61(9)
Co1–O4 <sup>#2</sup>	2.0193(19)	O2 <sup>#1</sup> –Co1–N5	88.25(8)
Co1–O3	2.037(2)	O4 <sup>#2</sup> –Co1–N5	95.73(9)
Co1–N1	2.189(3)	O3–Co1–N5	85.50(9)
Co1–N5	2.216(2)	N1–Co1–N5	173.67(9)
Co2–O6 <sup>#3</sup>	2.0072(19)	O6 <sup>#3</sup> –Co2–O5 <sup>#4</sup>	104.99(8)
Co2–O5 <sup>#4</sup>	2.013(2)	O6 <sup>#3</sup> –Co2–O7	152.30(8)
Co2–O7	2.080(2)	O5 <sup>#4</sup> –Co2–O7	102.32(8)
Co2–N8 <sup>#5</sup>	2.157(2)	O6 <sup>#3</sup> –Co2–N8 <sup>#5</sup>	89.87(8)
Co2–N4	2.175(2)	O5 <sup>#4</sup> –Co2–N8 <sup>#5</sup>	89.17(8)
O2 <sup>#1</sup> –Co1–O4 <sup>#2</sup>	103.86(8)	O7–Co2–N8 <sup>#5</sup>	85.94(8)
O2 <sup>#1</sup> –Co1–O3	109.18(9)	O6 <sup>#3</sup> –Co2–N4	96.66(9)
O4 <sup>#2</sup> –Co1–O3	146.96(9)	O5 <sup>#4</sup> –Co2–N4	91.18(9)
O2 <sup>#1</sup> –Co1–N1	91.50(8)	O7–Co2–N4	87.29(8)
O4 <sup>#2</sup> –Co1–N1	90.47(9)	N8 <sup>#5</sup> –Co2–N4	173.13(9)

Symmetry equivalent positions: #1 –*x*, –*y* + 1, –*z*; #2 *x* – 1, *y*, *z* + 1; #3 *x* + 1, *y* + 1, *z*; #4 –*x* + 2, –*y* + 2, –*z* – 1; #5 *x* + 2, *y* + 1, *z* – 1.

(OCO)<sub>2</sub> dimeric kernels, which have a Co...Co contact separation of 4.557 Å. These are connected into 1D [Co(OHip)]<sub>n</sub> ribbons (Fig. 1), which are oriented parallel to the [0 1 1] crystal direction.

The [Co(OHip)]<sub>n</sub> ribbons are connected into [Co(OHip)(4-bpmp)]<sub>n</sub> 2D coordination polymer layers (Fig. 2a) by 4-bpmp ligands that conjoin Co1 and Co2 atoms in neighboring ribbons, with a Co...Co through-ligand distance of 15.843 Å. Individual [Co(OHip)(4-bpmp)]<sub>n</sub> layers are oriented parallel to the (1 –1 1) crystal planes. The angle between the pyridyl nitrogen atoms and the piperazinyl ring centroid (defined as  $\kappa$ ) is 170.4°. This slight kink results in a smaller through-ligand metal–metal distance than seen in other coordination polymers with “splayed-open” 4-bpmp ligands [36]. If the {Co<sub>2</sub>(OCO)<sub>2</sub>} dimers are considered to be the simplest connecting nodes, the underlying topology of the 2D net of **1** is that of a standard (4,4) rhomboid grid (Fig. 2b). Interlayer hydrogen bonding interactions (Table 3) between the hydroxy

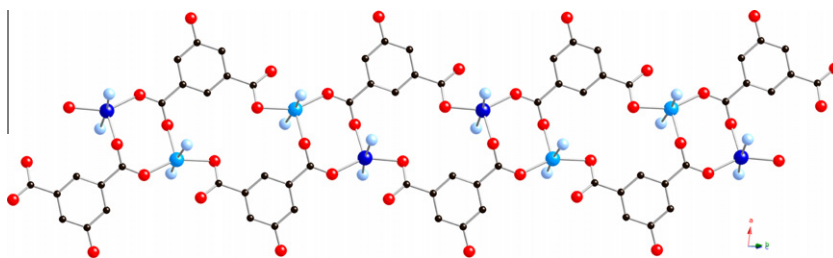


Fig. 1.  $[\text{Co}(\text{OHip})]_n$  ribbon in **1**.

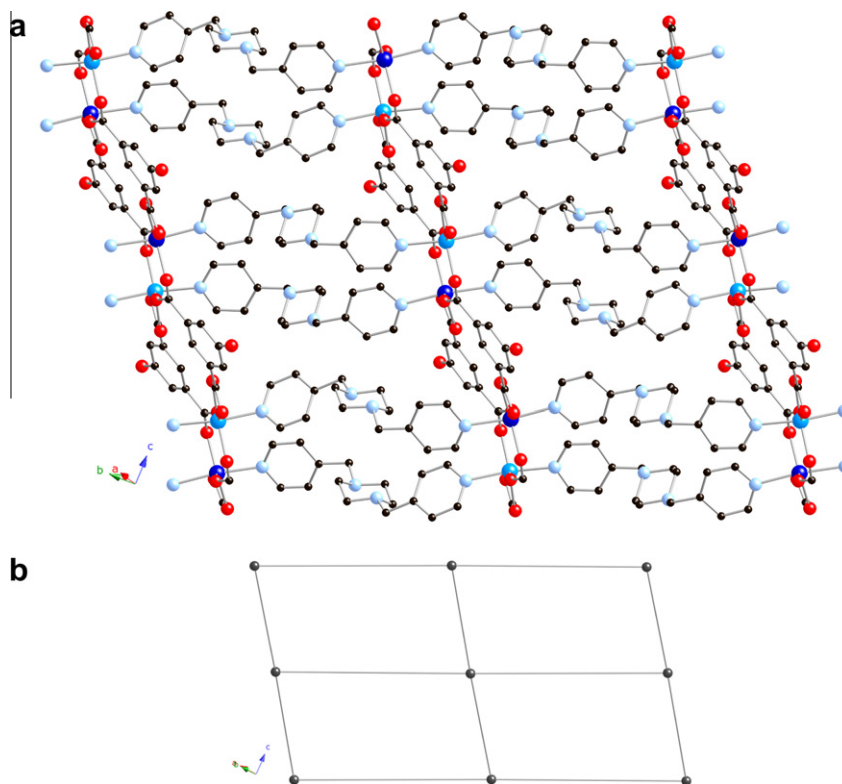


Fig. 2. (a)  $[\text{Co}(\text{OHip})(4\text{-bpmp})]_n$  coordination polymer layer in **1**. (b) Schematic perspective of the underlying (4,4) grid topology of **1**, with the dimeric  $\{\text{Co}_2(\text{OCO})_2\}$  connecting nodes represented as spheres.

**Table 3**  
Hydrogen bonding distance (Å) and angle ( $^\circ$ ) data for **1–3**.

D–H...A	$d(\text{H}\cdots\text{A})$	DHA	$d(\text{D}\cdots\text{A})$	Symmetry transformation for A
<b>1</b>				
O9–H9O...O1	2.07(3)	168(4)	2.799(3)	$-x + 1, -y + 1, -z$
O10–H10O...O8	2.08(3)	162(4)	2.790(3)	$-x + 3, -y + 2, -z - 1$
<b>3</b>				
O1–H1A...O5	1.794(19)	175(3)	2.652(4)	
O1–H1B...O2	2.28	174.5	3.096(5)	$-x, -y, -z$
O1W–H1WA...O6	1.94(2)	173(9)	2.800(6)	
O2–H2A...O6	1.82(2)	176(5)	2.661(4)	
O2–H2B...O3W	1.96(2)	167(5)	2.795(6)	$-x, -y, -z - 1$
O2W–H2WB...O1	1.89	161.3	2.724(7)	$x, y, z - 1$
O3W–H3WA...O8	2.16	179.1	3.009(7)	$x, y - 1, z$
O3W–H3WB...O3	1.95	179.0	2.798(6)	
N2–H2 N...O4	1.65(2)	171(5)	2.547(5)	$x + 2, y - 1, z + 1$

groups of the OHip ligands and the semi-ligating carboxylate oxygen atoms serves to aggregate the  $[\text{Co}(\text{OHip})(4\text{-bpmp})]_n$  layers into the pseudo 3D crystal structure of **1**. The topology of **1** also contrasts with the fourfold interpenetrated  $6^6$  diamondoid net seen in its dpp analog [13].

#### 4.3. Structural description of $[\text{Co}(\text{O}Meip)(4\text{-bpmp})]_n$ (**2**)

The asymmetric unit of compound **2** contains a divalent cobalt atom, a fully deprotonated OMeip ligand, and a 4-bpmp ligand. The coordination environment about cobalt is a distorted  $\{\text{CoN}_2\text{O}_4\}$

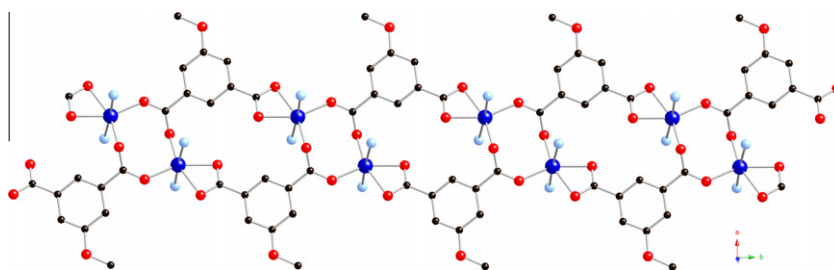
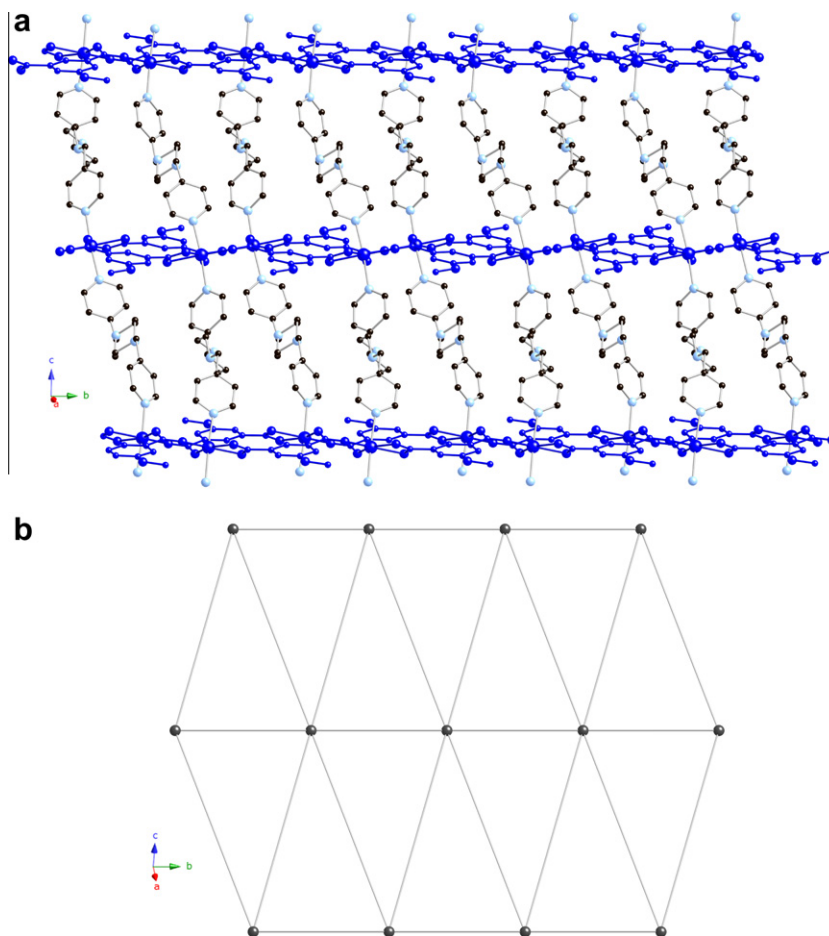
**Table 4**Bond length (Å) and angle (°) data for **2**.

Co1–O5	2.015(2)	O2 <sup>#2</sup> –Co1–O1 <sup>#2</sup>	60.92(8)
Co1–O4 <sup>#1</sup>	2.047(2)	O5–Co1–N4	89.09(9)
Co1–O2 <sup>#2</sup>	2.149(2)	O4 <sup>#1</sup> –Co1–N4	97.05(9)
Co1–O1 <sup>#2</sup>	2.180(2)	O2 <sup>#2</sup> –Co1–N4	89.22(9)
Co1–N4	2.192(3)	O1 <sup>#2</sup> –Co1–N4	91.63(9)
Co1–N3 <sup>#3</sup>	2.194(3)	O5–Co1–N3 <sup>#3</sup>	88.80(9)
O5–Co1–O4 <sup>#1</sup>	104.54(9)	O4 <sup>#1</sup> –Co1–N3 <sup>#3</sup>	88.17(9)
O5–Co1–O2 <sup>#2</sup>	98.03(9)	O2 <sup>#2</sup> –Co1–N3 <sup>#2</sup>	86.28(9)
O4 <sup>#1</sup> –Co1–O2 <sup>#2</sup>	156.63(8)	O1 <sup>#2</sup> –Co1–N3 <sup>#3</sup>	88.60(9)
O5–Co1–O1 <sup>#2</sup>	158.91(9)	N4–Co1–N3 <sup>#3</sup>	174.71(10)
O4 <sup>#1</sup> –Co1–O1 <sup>#2</sup>	96.29(8)		

Symmetry equivalent positions: #1  $-x, -y + 1, -z$ ; #2  $-x, -y + 2, -z$ ; #3  $x + 1, -y + 3/2, z - 1/2$ .

octahedron with pyridyl nitrogen donor atoms from two 4-bmpm ligands situated *trans* to each other. A chelating carboxylate group from an OMeip ligand occupies two of the equatorial sites, while *cis* disposed single carboxylate oxygen atom from two different OMeip ligands fill the remaining two equatorial positions. The six-coordinate geometry about cobalt in **2** contrasts with the “5+1” square pyramidal environment in its OHip analog **1**. Pertinent bond data for **2** is listed in Table 4.

The OMeip ligands bridge three cobalt atoms, like in **1**, but in a  $\kappa^4\text{O}_2\text{O}'\text{O}''$  ligating mode because of the chelation of one carboxylate terminus. As in **1**, the other carboxylate arm bridges two cobalt atoms in an *anti-syn* manner to construct  $\{\text{Co}_2(\text{OCO})_2\}$  dimeric kernels, which have a Co...Co contact separation of 4.527 Å. The slight decrease in Co...Co distance in **2** is ascribed to the chelat-

**Fig. 3.**  $[\text{Co}(\text{OMeip})]_n$  ribbon in **2**.**Fig. 4.** (a)  $[\text{Co}(\text{OMeip})(4\text{-bpm})]_n$  coordination polymer layer in **2**. (b) Schematic perspective of the underlying (3,6) grid topology of **2**, with the dimeric  $\{\text{Co}_2(\text{OCO})_2\}$  connecting nodes represented as spheres.

ing binding mode of the non-bridging carboxylate group, as opposed to the monodentate binding mode seen in the OHip derivative **1**. The full span of the OMeip ligands connects neighboring  $\{\text{Co}_2(\text{OCO})_2\}$  dimers into 1D  $[\text{Co}(\text{OMeip})]_n$  ribbons (Fig. 3), which are oriented parallel to the  $[0\ 1\ 0]$  crystal direction.

Parallel  $[\text{Co}(\text{OMeip})]_n$  ribbons are connected into  $[\text{Co}(\text{OMeip})(4\text{-bpmp})]_n$  2D coordination polymer layers (Fig. 4a) by 4-bpmp ligands that span a Co...Co through-ligand distance of 15.898 Å. Individual layers lie parallel to the  $(1\ 0\ 2)$  crystal planes. The  $\kappa$  angle between the pyridyl nitrogen atoms and the piperazinyl ring centroid is 173.8°; this more open angle results in a slightly longer Co...Co distance than seen in **1**.

Similar to the pattern seen in **1**, each  $\{\text{Co}_2(\text{OCO})_2\}$  dimer connects to two others along a single  $[\text{Co}(\text{OMeip})]_n$  ribbon. However, in marked contrast to **1**, 4-bpmp ligands connect each  $\{\text{Co}_2(\text{OCO})_2\}$  dimer to four others, two in each neighboring  $[\text{Co}(\text{OMeip})]_n$  ribbon. Thus rarer (3,6) triangular grids (Fig. 4b) [37] are formed in **2**, in contrast to the (4,4) grids in **1**. It is plausible that the increased steric bulk and lack of hydrogen-bonding ability of the methoxy substituent, in addition to the adjustment of carboxylate binding mode, results in the significant change in underlying layer topology between **1** and **2**. A (3,6) triangular net is seen in  $[\text{Co}(\text{ip})(4\text{-bpmp})]_n$ , the unsubstituted analog of **2** [38], which also lacks substituent induced hydrogen bonding. Adjacent  $[\text{Co}(\text{OMeip})(4\text{-bpmp})]_n$  layers stack in an AAA pattern along the  $a$  crystal direction by crystal packing forces to generate the pseudo 3D structure of **2**.

#### 4.4. Structural description of $[\{\text{Co}(\text{H}_2\text{O})_4(\text{H}_2\text{3-bpmp})\}(\text{NO}_2\text{ip})_2 \cdot 6\text{H}_2\text{O}]_n$ (**3**)

The asymmetric unit of compound **3** contains a cobalt atom on a crystallographic inversion center, two aqua ligands, one-half of a 3-

**Table 5**  
Bond length (Å) and angle (°) data for **3**.

Co1–O2 <sup>#1</sup>	2.109(3)	O2–Co1–O1 <sup>#1</sup>	94.28(13)
Co1–O2	2.109(3)	O1–Co1–O1 <sup>#1</sup>	180.0
Co1–O1	2.115(3)	O2 <sup>#1</sup> –Co1–N1	88.44(13)
Co1–O1 <sup>#1</sup>	2.115(3)	O2–Co1–N1	91.56(13)
Co1–N1	2.145(3)	O1–Co1–N1	91.06(12)
Co1–N1 <sup>#1</sup>	2.145(3)	O1 <sup>#1</sup> –Co1–N1	88.94(12)
O2 <sup>#1</sup> –Co1–O2	180.0(2)	O2 <sup>#1</sup> –Co1–N1 <sup>#1</sup>	91.56(13)
O2 <sup>#1</sup> –Co1–O1	94.28(13)	O2–Co1–N1 <sup>#1</sup>	88.44(13)
O2–Co1–O1	85.72(13)	O1–Co1–N1 <sup>#1</sup>	88.94(12)
O2 <sup>#1</sup> –Co1–O1 <sup>#1</sup>	85.72(13)	O1 <sup>#1</sup> –Co1–N1 <sup>#1</sup>	91.06(12)

Symmetry equivalent position: #1  $-x, -y, -z$ .

bpmp ligand protonated at its piperazinyl nitrogen atoms, an unligated  $\text{NO}_2\text{ip}$  dianion, and three water molecules of crystallization. A  $[\text{CoN}_2\text{O}_4]$  coordination octahedron is present in **3**, with *trans* pyridyl nitrogen donor atoms from two  $\text{H}_2\text{3-bpmp}^{2+}$  ligands and four aqua ligands. Bond lengths and angles within the coordination sphere are consisted with octahedrally coordinated cobalt (Table 5).

The  $\text{H}_2\text{3-bpmp}^{2+}$  ligands connect  $[\text{Co}(\text{H}_2\text{O})_4]^{2+}$  fragments into  $[\text{Co}(\text{H}_2\text{O})_4(\text{H}_2\text{3-bpmp})]_n^{4n+}$  coordination polymer chain motifs (Fig. 5a), with Co...Co contact distances of 13.594 Å. This distance is much shorter than the related metal–metal contact distances in **1** and **2**, because of the kinked disposition of the 3-position pyridyl nitrogen donors in the isomeric variant of 4-bpmp. The  $\text{H}_2\text{3-bpmp}^{2+}$  ligands are restricted by crystallographic symmetry to adopt an *anti* conformation (N...N...N...N dihedral angle = 180°). Parallel  $[\text{Co}(\text{H}_2\text{O})_4(\text{H}_2\text{3-bpmp})]_n^{4n+}$  chains are organized into the 3D crystal structure of **3** by numerous hydrogen bonding pathways involving unligated water molecules and  $\text{NO}_2\text{ip}$  dianions (Fig. 5b). A very similar chain motif was seen in  $[\{\text{Co}(\text{H}_2\text{O})_4(\text{H}_2\text{3-bpmp})\}(1,3\text{-phda})_2 \cdot 8\text{H}_2\text{O}]_n$  (1,3-phda = 1,3-phenylenediacetate) [39], showing a structural invariance to the nature of the unligated aromatic dicarboxylate. The water molecules of crystallization in **3** occupy 15.0% of the unit cell volume, as determined with PLATON software [40]. In contrast to two previously reported 2D cobalt coordination polymers containing both  $\text{NO}_2\text{ip}$  and dipyrindine moieties, the  $\text{NO}_2\text{ip}$  ions do not engage in ligation in **3**. It is plausible that the surfeit of aqua ligands and water molecules of crystallization provide enough stability from supramolecular hydrogen bonding pathways to prevent  $\text{NO}_2\text{ip}$  ligation.

#### 4.5. Variable temperature magnetic properties of **1** and **2**

Variable temperature magnetic data were recorded for polycrystalline samples of **1** and **2** in order to probe possible magnetic superexchange within their respective  $\{\text{Co}_2(\text{OCO})_2\}$  dimeric subunits. The phenomenological Rueff expression [41] (Eq. (1)) has been successfully applied in the recent past to  $S = 3/2$  dimers [42]. This treatment is necessary because of the significant cooperative effects of magnetic coupling ( $J$ ) and single ion effects such as zero-field splitting ( $D$ ) on variable temperature magnetic behavior.

$$\chi_m T = A \exp(-D/kT) + B \exp(J/kT), \text{ where } A + B + C = (5 \text{ Ng}^2 \beta^2 / 4k) \quad (1)$$

The best-fit values to Eq. (1) for the (4,4) grid topology OHip coordination polymer **1** (Fig. 6a) were  $A = 1.06(4) \text{ cm}^3 \text{ K mol Co}^{-1}$  and  $B = 2.39(2) \text{ cm}^3 \text{ K mol Co}^{-1}$  giving  $g = 2.71(4)$ ,  $J = 0.32(3) \text{ cm}^{-1}$

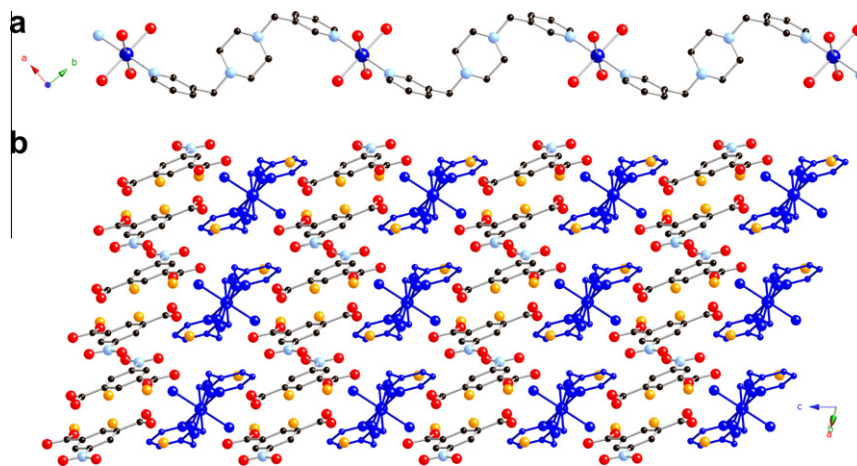


**Fig. 5.** (a)  $[\text{Co}(\text{H}_2\text{O})_4(\text{H}_2\text{3-bpmp})]_n^{4n+}$  coordination polymer chain in **3**. (b) Stacking of chains in **3** via unligated  $\text{NO}_2\text{ip}$  dianions and water molecules.

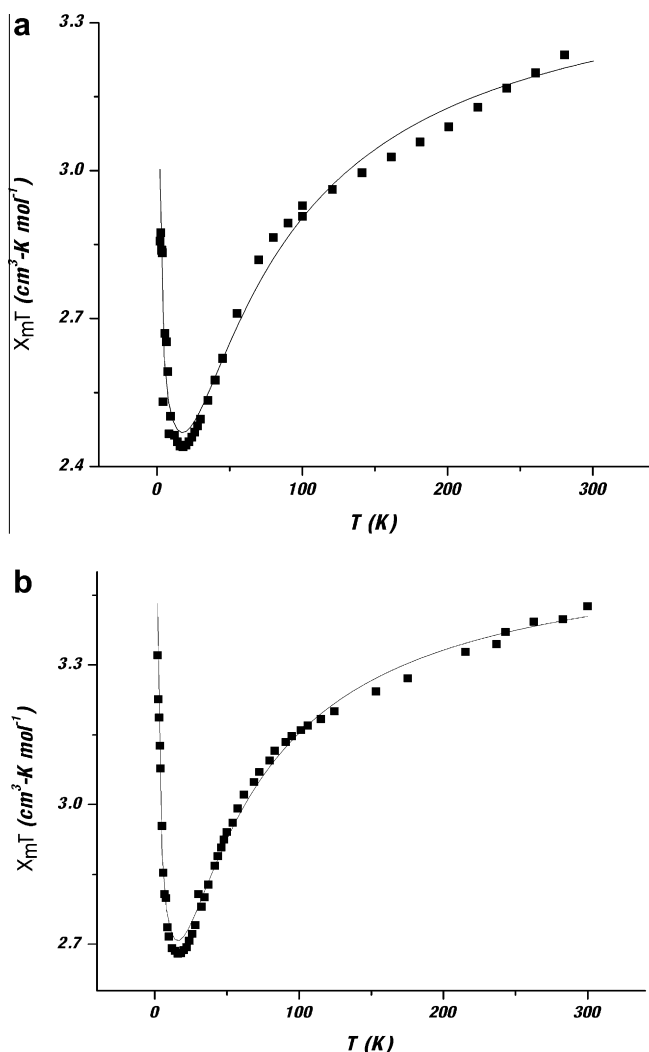


**Fig. 6.** Variable temperature magnetic plots for (a) **1** and (b) **2**. The best-fit to the Ruff phenomenological expression (Eq. (1)) is shown as a thin line in each graph.

and  $D = 52(5) \text{ cm}^{-1}$ , with  $R = 3.1 \times 10^{-3} = \{\Sigma[(\chi_m T)_{\text{obs}} - (\chi_m T)_{\text{calc}}]^2 / \Sigma[(\chi_m T)_{\text{obs}}]^2\}$ . The decrease in  $\chi_m T$  product between 300 and 18 K is ascribed to the generation of  $S = 1/2$  Kramers doublet states because of zero field splitting. The small, positive  $J$  value indicates weak ferromagnetic coupling between  $d^7 \text{ Co}^{2+}$  ions in the  $\{\text{Co}_2(\text{OCO})_2\}$  dimeric subunits, manifested by the upturn in the value of the  $\chi_m T$  product below 18 K.

The best-fit values to Eq. (1) for the (3,6) grid topology OMeip coordination polymer **2** (Fig. 6b) were  $A = 0.98(2) \text{ cm}^3 \text{ K mol Co}^{-1}$  and  $B = 2.59(2) \text{ cm}^3 \text{ K mol Co}^{-1}$  giving  $g = 2.68(2)$ ,  $J = 0.39(2) \text{ cm}^{-1}$  and  $D = 40(2) \text{ cm}^{-1}$ , with  $R = 1.2 \times 10^{-3}$ . As for **1**, the decrease in  $\chi_m T$  product between 300 and 20 K is attributed to the formation of  $S = 1/2$  Kramers doublet states driven by zero field splitting. Again the small, positive  $J$  value is a sign of weak ferromagnetic coupling within the  $\{\text{Co}_2(\text{OCO})_2\}$  dimeric subunits. This is manifested by the increase in the  $\chi_m T$  product below 20 K. The slight increase in  $J$  in **2** could possibly arise from the shorter intradimer  $\text{Co} \cdots \text{Co}$  distance because of the chelating binding mode of the OMeip ligands. Elevated  $g$  values for divalent cobalt in distorted octahedral environments are common because of well-known spin-orbit coupling effects [28]. Still, the best-fit values for **1** and **2** should be taken as estimates because Eq. (1) is a phenomenological expression and not one derived rigorously from spin exchange Hamiltonians.

## 5. Conclusions

The hydrogen-bonding capability of 5-position substituents on isophthalate ligands appears to dictate topology during self-assembly of divalent cobalt coordination polymers containing neutral bis(pyridylmethyl)piperazine ligands. In both OHip and OMeip cases, one-dimensional “infinite”  $[\text{Co}(\text{dicarboxylate})]_n$  ribbons with embedded  $\{\text{Co}_2(\text{OCO})_2\}$  dimeric kernels are formed. However, the hydroxy group of the OHip ligands engages in hydrogen bonding to an OHip carboxylate group in another coordination polymer layer, enforcing adjustment of carboxylate binding mode. In turn a conformational change in the 4-bpmp ligand results in each  $\{\text{Co}_2(\text{OCO})_2\}$  dimer acting as a 4-connected node. In the case of the OMeip ligand, hydrogen bonding donation on the part of the 5-position substituent is no longer possible. The supramolecular environment then more closely resembles that of the unsubstituted isophthalate ligand despite the added steric hindrance, resulting in a (3,6) triangular net with  $\{\text{Co}_2(\text{OCO})_2\}$  dimers serving as 6-connected nodes. Because of their common  $\{\text{Co}_2(\text{OCO})_2\}$  dimeric units, both the OHip derivative **1** and OMeip derivative **2** display similar cooperativity between single-ion effects and weak carboxylate-mediated ferromagnetism. Both **1** and **2** and their unsubstituted isophthalate analog possess 2D topologies. In contrast, compound **3** adopts a 1D chain motif, likely because of the different nitrogen donor disposition within the 3-bpmp ligand.

## Acknowledgements

The authors gratefully acknowledge the donors of the American Chemical Society Petroleum Research Fund for financial support of this work. We thank Mr. Chaun I.B. Gandolfo for acquiring the infrared spectra.

## Appendix A. Supplementary material

CCDC 793894, 793892, and 793893 contain the supplementary crystallographic data for **1**, **2**, and **3**. These data can be obtained free of charge from The Cambridge Crystallographic Data Centre via [www.ccdc.cam.ac.uk/data\\_request/cif](http://www.ccdc.cam.ac.uk/data_request/cif). Supplementary data associated with this article can be found, in the online version, at [doi:10.1016/j.ica.2011.03.009](https://doi.org/10.1016/j.ica.2011.03.009).

## References

- [1] C. Janiak, *Dalton Trans.* 1 (2003) 2781 (and references therein).
- [2] U. Mueller, M. Schubert, F. Teich, H. Puetter, K. Schierle-Arndt, J. Pastré, *J. Mater. Chem.* 16 (2006) 626.
- [3] (a) L. Pan, D.H. Olson, L.R. Ciemnomlonski, R. Heddy, J. Li, *Angew. Chem., Int. Ed.* 45 (2006) 616;  
(b) M. Dinca, A.F. Yu, J.R. Long, *J. Am. Chem. Soc.* 128 (2006) 8904;  
(c) J.L.C. Roswell, O.M. Yaghi, *Angew. Chem., Int. Ed.* 44 (2005) 4670;  
(d) R. Matsuda, R. Kitaura, S. Kitagawa, Y. Kubota, R.V. Belosludov, T.C. Kobayashi, H. Sakamoto, T. Chiba, M. Takata, Y. Kawazoe, Y. Mita, *Nature* 436 (2005) 238;  
(e) A.C. Sudik, A.R. Millward, N.W. Ockwig, A.P. Côté, J. Kim, O.M. Yaghi, *J. Am. Chem. Soc.* 127 (2005) 7110;  
(f) X. Zhao, B. Xiao, A.J. Fletcher, K.M. Thomas, D. Bradshaw, M.J. Rosseinsky, *Science* 306 (2004) 1012;  
G. Férey, M. Latroche, C. Serre, F. Millange, T. Loiseau, A. Percheron-Guegan, *Chem. Commun.* (2003) 2976;  
(g) H. Li, M. Eddaoudi, M. O’Keeffe, O.M. Yaghi, *Nature* 402 (1999) 276.
- [4] (a) J.-R. Li, R.J. Kuppler, H.-C. Zhou, *Chem. Soc. Rev.* 38 (2009) 1477 (and references therein);  
(b) A. Cingolani, S. Galli, N. Masciocchi, L. Pandolfo, C. Pettinari, A. Sironi, *Chem. Eur. J.* 14 (2008) 9890;  
(c) J.S. Seo, D. Whang, H. Lee, S.I. Jun, J. Oh, Y.J. Jeon, K. Kim, *Nature* 404 (2000) 982.
- [5] (a) Q.-R. Fang, G.-S. Zhu, M. Xue, J.-Y. Sun, S.-L. Qiu, *Dalton Trans.* (2006) 2399;  
(b) X.-M. Zhang, M.-L. Tong, H.K. Lee, X.-M. Chen, *J. Solid State Chem.* 160 (2001) 118;  
O.M. Yaghi, H. Li, T.L. Groy, *Inorg. Chem.* 36 (1997) 4292.

- [6] (a) J.Y. Lee, O.K. Farha, J. Roberts, K.A. Scheidt, S.T. Nguyen, J.T. Hupp, *Chem. Soc. Rev.* 38 (2009) 1450 (and references therein);  
(b) L. Ma, C. Abney, W. Lin, *Chem. Soc. Rev.* 38 (2009) 1248;  
(c) S.G. Baca, M.T. Reetz, R. Goddard, I.G. Filippova, Y.A. Simonov, M. Gdaniec, N. Gerbeleu, *Polyhedron* 25 (2006) 1215;  
(d) H. Han, S. Zhang, H. Hou, Y. Fan, Y. Zhu, *Eur. J. Inorg. Chem.* 8 (2006) 1594;  
(e) C.-D. Wu, A. Hu, L. Zhang, W. Lin, *J. Am. Chem. Soc.* 127 (2005) 8940;  
(f) W. Mori, S. Takamizawa, C.N. Kato, T. Ohmura, T. Sato, *Micropor. Mesopor. Mater.* 73 (2004) 31;  
(g) N. Guillou, Q. Gao, P.M. Forster, J.S. Chang, M. Noguès, S.-E. Park, G. Férey, A.K. Cheetham, *Angew. Chem., Int. Ed.* 40 (2001) 2831.
- [7] (a) M.D. Allendorf, C.A. Bauer, R.K. Bhakta, R.J.T. Houk, *Chem. Soc. Rev.* 38 (2009) 1330;  
(b) J. He, J. Yu, Y. Zhang, Q. Pan, R. Xu, *Inorg. Chem.* 44 (2005) 9279;  
(c) S. Wang, Y. Hou, E. Wang, Y. Li, L. Xu, J. Peng, S. Liu, C. Hu, *New J. Chem.* 27 (2003) 1144;  
(d) L.G. Beauvais, M.P. Shores, J.R. Long, *J. Am. Chem. Soc.* 122 (2000) 2763.
- [8] (a) S. Zang, Y. Su, Y. Li, Z. Ni, Q. Meng, *Inorg. Chem.* 45 (2006) 174;  
(b) L. Wang, M. Yang, G. Li, Z. Shi, S. Feng, *Inorg. Chem.* 45 (2006) 2474.
- [9] X.-N. Cheng, W.-X. Zhang, Y.-Y. Lin, Y.-Z. Zheng, X.-M. Chen, *Adv. Mater.* 19 (2007) 1494.
- [10] J. Tao, M.L. Tong, X.M. Chen, *J. Chem. Soc., Dalton Trans.* (2000) 3669.
- [11] B. Chen, C. Liang, J. Yang, D.S. Contreras, Y.L. Clancy, E.B. Lobkovsky, O.M. Yaghi, S. Dai, *Angew. Chem., Int. Ed.* 45 (2006) 1390;  
(a) S.W. Lee, H.J. Kim, Y.K. Lee, K. Park, J.H. Son, Y. Kwon, *Inorg. Chim. Acta* 353 (2003) 151.
- [12] M. Kurmoo, *Chem. Soc. Rev.* 38 (2009) 1353 (and references therein).
- [13] X.J. Li, R. Cao, W.H. Bi, Y.Q. Wang, Y.L. Wang, X. Li, *Polyhedron* 24 (2005) 2955.
- [14] H.Y. He, Y.L. Zhou, Y. Hong, L.G. Zhu, *J. Mol. Struct.* 737 (2005) 97.
- [15] X.J. Li, X.Y. Wang, S. Gao, R. Cao, *Inorg. Chem.* 45 (2006) 1508.
- [16] R.K. Feller, A.K. Cheetham, *Dalton Trans.* (2008) 2034.
- [17] L.F. Ma, B. Li, X.Y. Sun, L.Y. Wang, Y.T. Fan, *Z. Anorg. Allgem. Chem.* 636 (2010) 1606.
- [18] Z.M. Wilseck, C.M. Gandolfo, R.L. LaDuca, *Inorg. Chim. Acta.* 363 (2010) 3951.
- [19] M. Du, Z.H. Zhang, Y.P. You, X.J. Zhao, *CrystEngComm* 10 (2008) 306.
- [20] J. Luo, M. Hong, R. Wang, R. Cao, L. Han, D. Yuan, Z. Lin, Y. Zhou, *Inorg. Chem.* 42 (2003) 4486.
- [21] Y. Liu, Q. He, X. Zhang, Z. Xue, C. Lv, *Acta Crystallogr., Sect. E64* (2008) m1605.
- [22] F. Wang, K.J. Deng, G.Y. Lai, L. Cao, L.L. Wen, D.F. Li, *J. Inorg. Organomet. Polym.* 19 (2009) 494.
- [23] L.K. Sposato, R.L. LaDuca, *Acta Crystallogr., Sect. E65* (2009) m1082.
- [24] D.S. Zhou, F.K. Wang, S.Y. Yang, Z.X. Xie, R.B. Huang, *CrystEngComm* 11 (2009) 2548.
- [25] D.P. Martin, R.M. Staples, R.L. LaDuca, *Inorg. Chem.* 47 (2008) 9754.
- [26] G.A. Farnum, R.L. LaDuca, *Cryst. Growth Des.* 10 (2010) 1897.
- [27] L.L. Johnston, D.P. Martin, R.M. Supkowski, R.L. LaDuca, *Inorg. Chim. Acta* 361 (2008) 2887.
- [28] G.A. Farnum, J.S. Lucas, C.Y. Wang, R.L. LaDuca, *Inorg. Chim. Acta.* 368 (2011) 84.
- [29] D. Pocić, J.-M. Planeix, N. Kyritsakas, A. Jouaiti, M.W. Hosseini, *CrystEngComm* 7 (2005) 624.
- [30] O. Kahn, *Molecular Magnetism*, VCH Publishers, New York, 1993.
- [31] SAINT, Software for Data Extraction and Reduction, Version 6.02, Bruker AXS, Inc., Madison, WI, 2002.
- [32] SADABS, Software for Empirical Absorption Correction, Version 2.03, Bruker AXS, Inc., Madison, WI, 2002.
- [33] G.M. Sheldrick, *SHELXTL*, Program for Crystal Structure Refinement, University of Göttingen, Göttingen, Germany, 1997.
- [34] A.W. Addison, T.N.J. Rao, J. Reedijk, J. van Rijn, G.C. Verschoor, *J. Chem. Soc., Dalton Trans.* (1984) 1349.
- [35] J.W. Steed, D.A. Tocher, *Polyhedron* 13 (1994) 167.
- [36] D.P. Martin, R.M. Supkowski, R.L. LaDuca, *Dalton Trans.* (2009) 514.
- [37] (a) C.-Y. Su, Y.-P. Cai, C.-L. Chen, B.-S. Kang, *Inorg. Chem.* 40 (2001) 2210;  
D.L. Long, A.J. Blake, N.R. Champness, M. Schröder, *Chem. Commun.* (2000) 2273;  
(b) W. Lin, Z. Wang, L. Ma, *J. Am. Chem. Soc.* 121 (1999) 11249;  
(c) R. Bronisz, *Inorg. Chem.* 44 (2005) 4463;  
(d) J.-R. Li, X.-H. Bu, *Eur. J. Inorg. Chem.* (2008) 27;  
(e) Y. Qi, Y.-X. Che, J.-M. Zheng, *CrystEngComm* 10 (2008) 1137.
- [38] D.P. Martin, M.A. Braverman, R.L. LaDuca, *Cryst. Growth Des.* 7 (2007) 2609.
- [39] K.M. Blake, L.L. Johnston, M.A. Braverman, J.H. Nettleman, L.K. Sposato, R.L. LaDuca, *Inorg. Chim. Acta.* 363 (2010) 2233.
- [40] A.L. Spek, *PLATON*, A Multipurpose Crystallographic Tool, Utrecht University, Utrecht, The Netherlands, 1998.
- [41] J.M. Rueff, N. Masciocchi, P. Rabu, A. Sironi, A. Skoulios, *Chem. Eur. J.* 8 (2002) 1813.
- [42] J.H. Nettleman, R.M. Supkowski, R.L. LaDuca, *J. Solid State Chem.* 183 (2009) 291.